Journal of Sol-Gel Science and Technology (2024) 112:502–511
https://doi.org/10.1007/s10971-024-06548-w

ORIGINAL PAPER

Metal alkoxides as models for metal oxides—the concept revisited

Vadim G. Kessler[1]

Received: 15 August 2024 / Accepted: 5 September 2024 / Published online: 14 September 2024

Abstract

Sol-Gel synthesis of metal oxides constitutes a tremendously exciting domain of inorganic chemistry, where molecular and supramolecular science meet the physical chemistry and materials science. Structure and reactivity, especially surface complexation of biologically important molecules on the surface of metal oxide nanoparticles can efficiently be traced through structural studies of metal oxo-paperbags—the product of partial hydrolysis of alkoxide precursors. Paperbag is a recently proposed term to denote oligonuclear complexes not featuring intrinsic metal-metal bonding and thus not qualified to be called "clusters". Another important insight, provided recently by the studies of heterometallic species, is dealing with visualization of bonding modes of single atom catalysts on metal oxide substrates and reveals possible coordination environments of heteroatoms on doping. The studies of large paperbag aggregates can contribute to understanding of factors influencing the bandgap and photocatalytic activity of related oxides. The use of these species directly as photo or electro catalysts is rather debatable, however, in the view of high reactivity of these alkoxide intermediates, easily transforming them into metal oxide nanoparticles on hydrolysis or thermolysis.

Graphical Abstract

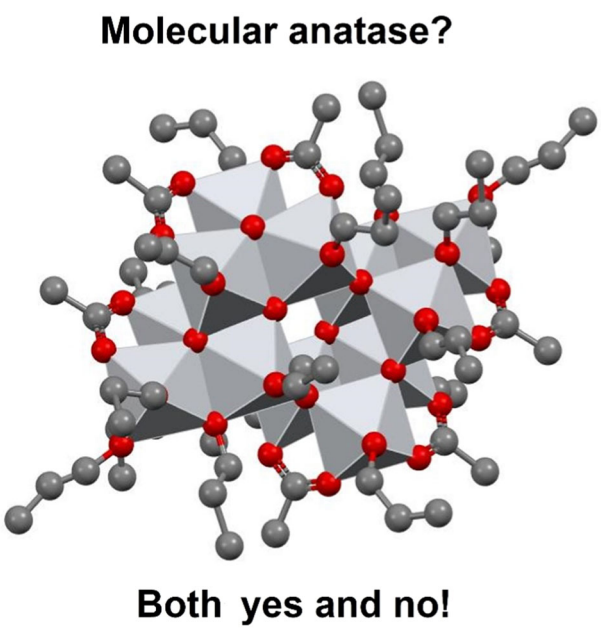

✉ Vadim G. Kessler
vadim.kessler@slu.se

[1] Department of Molecular Sciences, BioCenter, Swedish University of Agricultural Sciences, SE-75007 Uppsala, Sweden

Keywords Sol-Gel · Metal oxide · hydrolysis-polycondensation · metal oxo-paperbags (MOP) · surface structure models

Highlights

- Metal alkoxides form easily Oligonuclear Alkoxide Complexes, OAC, with metal-oxygen core structures resembling those of metal oxides.
- The structures of OAC result from two major factors – dense packing of cations and anions, and minimization of the surface energy.
- OAC provide good insights into redox reaction mechanisms of metal oxide nanoparticles and in coordination of surface-implanted heteroatoms.
- OAC are not clusters but paperbags, making direct studies of their reactivity in aqueous medium challenging.

1 Introduction

Metal alkoxides are salts of metal cations and alkoxide anions, RO^-, derived from alcohols that are extremely weak organic acids [1, 2]. This results in strong Brönsted and Lewis basicity of this class of compounds broadly used as basic catalysts [3]. The extreme basicity of the alkoxide ligands leads in many cases to formation of oligonuclear aggregates even for homoleptic alkoxides, i.e. derived from solely one kind of RO^- ligand.

Majority of oxo-alkoxides, where part of the ligands are replaced by an even more basic oxide ligand, O^{2-}, are complexes comprising several metal centers. Major input into bonding in these compounds is, just as in the structures of metal oxides, done by electrostatic interactions between cations and the oxygen atoms, permitting thus to consider these molecular aggregates as fragments of oxide structure terminated by alkyl groups [4].

Another factor shaping the oligonuclear metal alkoxides is the general trend for minimization of surface energy, leading to spheroidal or ellipsoidal topology [5]. It is rather important to note that the structures of metal (oxo)alkoxides are very often closely resembling those of polyoxometalate ions (POMs), following the Pauling's principles of mineral oxide network construction [6] and obeying the minimum surface energy trend. Oligonuclear metal complexes are often called "clusters", but this term is not correct in applying to oligonuclear species not featuring metal-metal bonds [7] such as metal alkoxides and POMs and thus a new term Metal-Oxo-Paperbags (MOP) has been established [8] and will be used further in this review. MOP resemble metal oxide nanoparticles (NP) and at present are probably most interesting as molecular level defined models of NP surface and reactivity, including redox properties, incorporation of single atom catalytic centers, ligand attachment to surface, ligand influence on the bandgap structure etc.

2 Analysis and discussion

2.1 General structural principles

The structures of oligonuclear alkoxide complexes (OAC) and MOP in general can be seen in the light of Bradley's structure theory [9] and Pauling's principles of mineral construction [6], both underlying the importance of stable coordination polyhedrons, resulting from critical radius ratios between cation and surrounding anions. The other important point identified by Pauling is the need to maximize the distance between highly charged cations in the structure, resulting in lower stability of edge sharing fragments compared to corner sharing and even less – for the face sharing ones. In fact, the face sharing in metal alkoxides has only been proved to exist in true clusters containing metal-metal bonds, such as, for example, $Re_2O_3(OMe)_6$ [10] or $ReMoO_2(OMe)_7$ [11] (Fig. 1A, B). The other trend is, of course, the densest possible packing of metal cations and ligands in the structure [12]. This results in two octahedra sharing an edge, a M_2O_{10} core, being the most common structure for binuclear OAC, exemplified by $[M(O^iPr)_4(^iPrOH)]_2$ (M = Zr, Hf, Sn(IV), see Fig. 1C [13, 14]) or $M_2O_2(OMe)_8$ (M = Mo [15], W [16], see Fig. 1D). Three octahedrons sharing edges in a triangle, a M_3O_{13}, is the most common building block in both OAC and POM structures and is often observed in oxo-alkoxides of Ti, Zr, Hf [17, 18] (Fig. 1E).

Its extension into an infinite flat layer analogous to the layered double hydroxide (LDH) structure is the case of $M(OR)_2$ with primary alkoxide ligands, where low-charged and relatively small (!) M^{2+}-cations can occupy all the neighboring places [2] (Fig. 2).

The molecular construction of LDH formed on hydrolysis of nickel precursors has been confirmed in the work of Ira Weinstock where it was complexed on the surface by POM species [19]. If we look closer at general trends in OAC structure build-up, it can be noticed that the M_3O_{13} triangle is typical as a building block for high-valent cation structures at

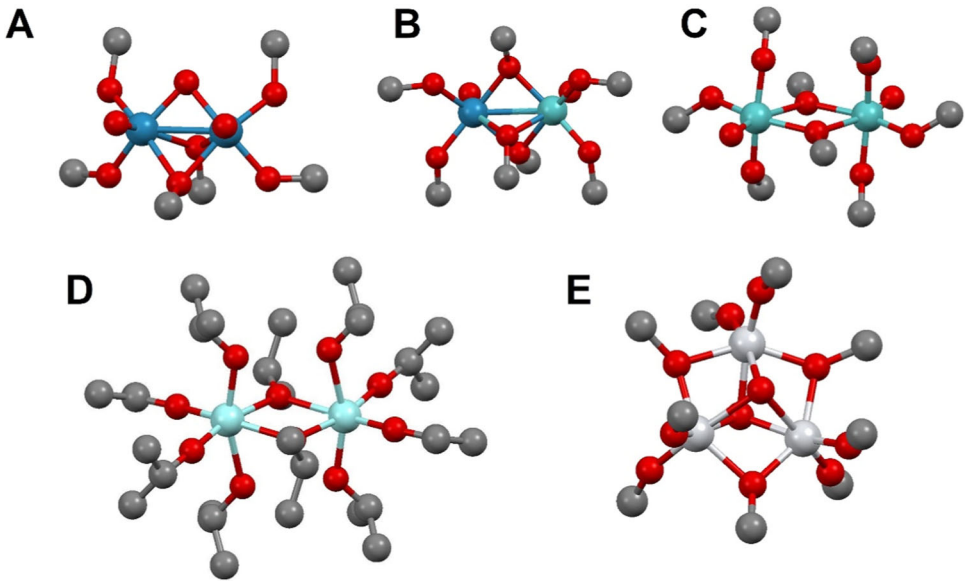

Fig. 1 Molecular structures of $Re_2O_3(OMe)_6$ (**A**) [10], $ReMoO_2(OMe)_7$ (Re in blue and Mo in turquoise, **B**) [11], $[M(O^iPr)_4(^iPrOH)]_2$ (M = Zr), Hf, Sn(IV) (**C**) [13, 14], $M_2O_2(OMe)_8$, M = Mo [15], W [16] (**D**) and $Ti_3O(O^iPr)_{10}$ (only central C-atom provided for clarity, disordered iPr bridging group not displayed, **E**) [17]

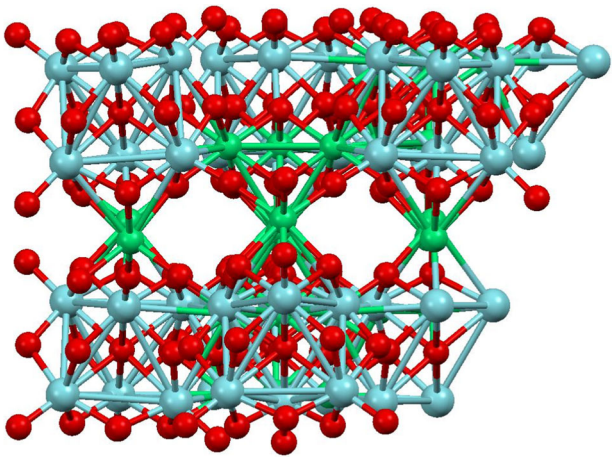

Fig. 2 Molecular structure of the $Ni(OH)_2$ LDH complex with $Nb_6O_{19}^{8-}$ anions [19]

lower hydrolysis ratios (oxo-ligand content) in Zr(IV) and Hf(IV) [20] (Fig. 3A), Nb(V) such as in oxo-alkoxides derivatives of linear chain alcohols, $Nb_8O_{10}(OR)_{20}$ [21, 22] (Fig. 3B) or Mo(VI) and W(VI) alkoxides and Lindquist and Keggin POMs [23, 24] (Fig. 3C). Additional factor seen apparently in the species with relatively low hydrolysis ratio/oxo-ligand substitution is the already mentioned trend to minimization of surface energy and steric hindrance, leading to placement of the alkyl chains on the surface of the aggregate, converting it into a hollow spheroid/ellipsoid. One of the most impressive examples of this trend is revealed in the structure of $(H_6[Ti_{42}(\mu_3\text{-}O)_{60}(O^iPr)_{42}(OH)_{12})]$ [25], which can be described as a layer of anatase structure rolled in into a sphere (Fig. 3D). At higher hydrolysis/oxo-substitution ratios the structures "collapse" and the core becomes more like a 3D oxide structure [23, 26]. For titanium near-complete hydrolysis at room temperature or in boiling water results in formation of uniform nanoparticles with most commonly anatase core structure that can be confirmed by either electron [27] or even X-ray diffraction [28].

Less charged cations permit denser packing in the core with square pyramidal M_5O building blocks for trivalent metal cations such as Al^{3+} [29], Fe^{3+} [30] and even Rare Earths (RE), Ln^{3+}, as in $Ln_5O(O^iPr)_{13}$ [31] (Fig. 4A). It is interesting to note that this kind of packing looks as resembling that in NaCl structure type, not related to the oxide or hydroxide structures for these elements. For large cations of divalent elements the structures of OAC can be resembling that of the corresponding oxide for Ca^{2+} as in $[Ca_6(\mu_4\text{-}0)_2(\mu_3\text{-}0Et)_4(\{0Et\})_4]\cdot 14EtOH$, featuring a NaCl type packing (as in CaO, see Fig. 4B) [32], or display a fluorite type packing with even larger cations such as Sr^{2+}, Ba^{2+} and even Sn^{2+} (Fig. 4C) [33].

It can thus be concluded, that the analogy between the structures of oligonuclear alkoxides and those of the corresponding oxides not always can be traced. The case of lucky coincidence, serendipity, is observed, however, for one of the most important oxide materials, titanium dioxide (as anatase), opening a perspective for experimental molecular modeling of its surface and even bulk properties [34].

2.2 Modeling of redox properties

Visualization of redox transformations of metal oxides was actually the topic of the very first publication, formulating the concept by Malcolm Chisholm et al. [4]. The focus was on understanding of transformations in metal-metal bonding, especially the fate of a localized multiple bond [35] (see Fig. 5).

An exciting challenge would be to model the redox properties of a metal oxide NP, applying an OAC as model.

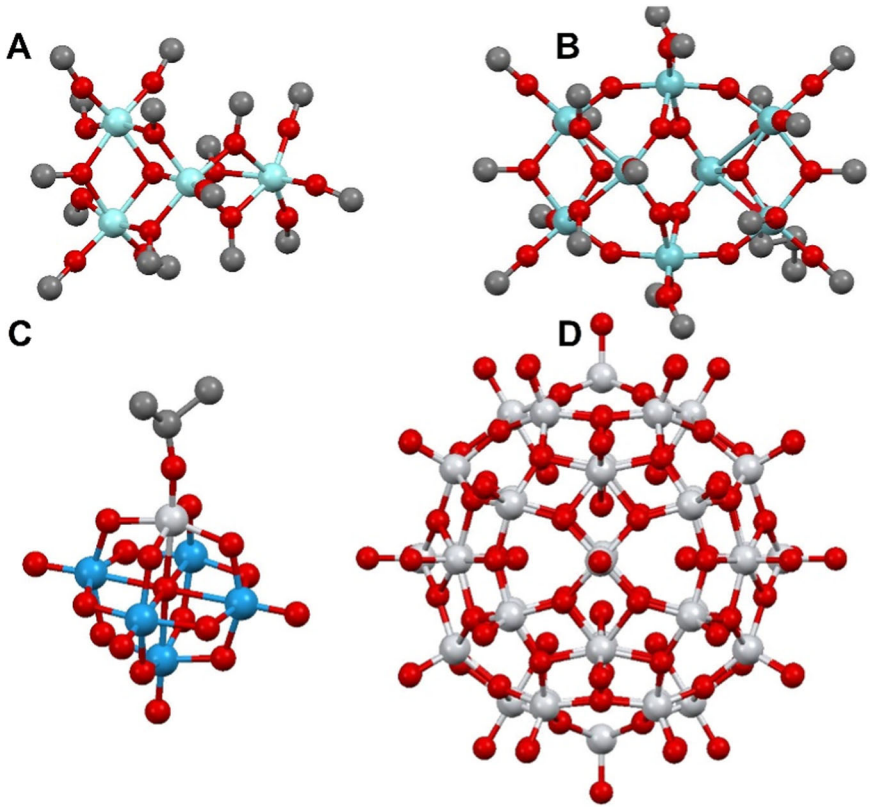

Fig. 3 Molecular structures of $Zr_4O(O^nPr)_{14}$ (**A**) [20], $Nb_8O_{10}(OR)_{20}$ (**B**) [21, 22] only first carbon atom of the ligand displayed for clarity, Lindqvist-$W_5TiO_{18}(O^iPr)^{3-}$ anion [24] (**C**) and ($H_6[Ti_{42}(\mu_3\text{-}O)_{60}(O^iPr)_{42}(OH)_{12}$)] (**D**) [25] (no carbon atoms were actually securely located in the reported model)

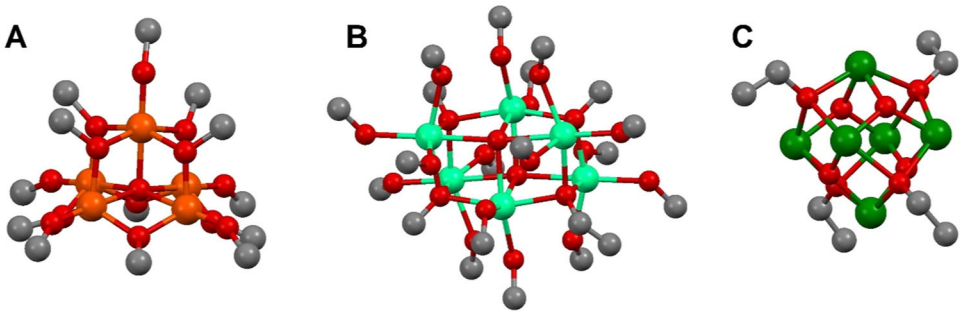

Fig. 4 Molecular structures of $Fe_5O(OEt)_{13}$ (**A**) [30], $[Ca_6(\mu_4\text{-}0)_2(\mu_3\text{-}0Et)_4(\{0Et\})_4]\cdot 14EtOH$ (**B**) [32]—only first carbon atoms of the ethyl group retained for clarity, and $Sn_6O_4(OEt)_4$ (**C**) [33]

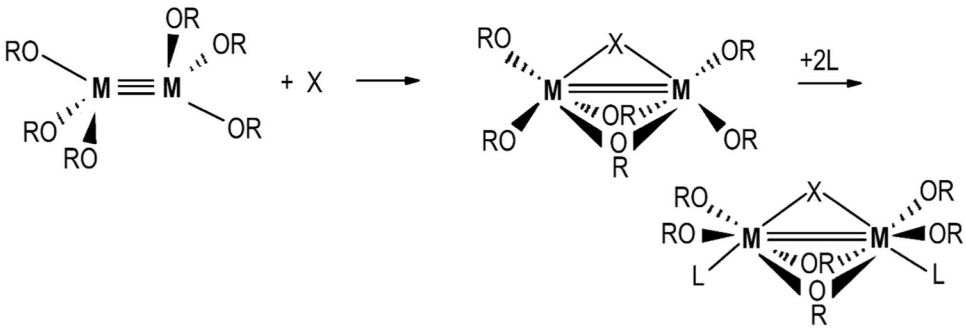

Fig. 5 Transformations of a triple W≡W bond in reactions of the tungsten alkoxides (after [35]), M = Mo, W; X = CO, HCCH; L = Py, $HNMe_2$

Attention in the recent years has been set on protein corona phenomenon [36] and oxidation of specific amino acids. Possible hinder lies in facile oxidation of the alkoxide ligand itself, reducing the choice of possible meaningful substrates and the sensitivity of alkoxides to hydrolysis in the view that the reactions of interest occur usually in aqueous media. The research in this direction is on-going in our group and at least POM species also belonging to the MOP family have already successfully been applied for visualizing of, in particular, specific tryptophan oxidation pathways [37]. It was

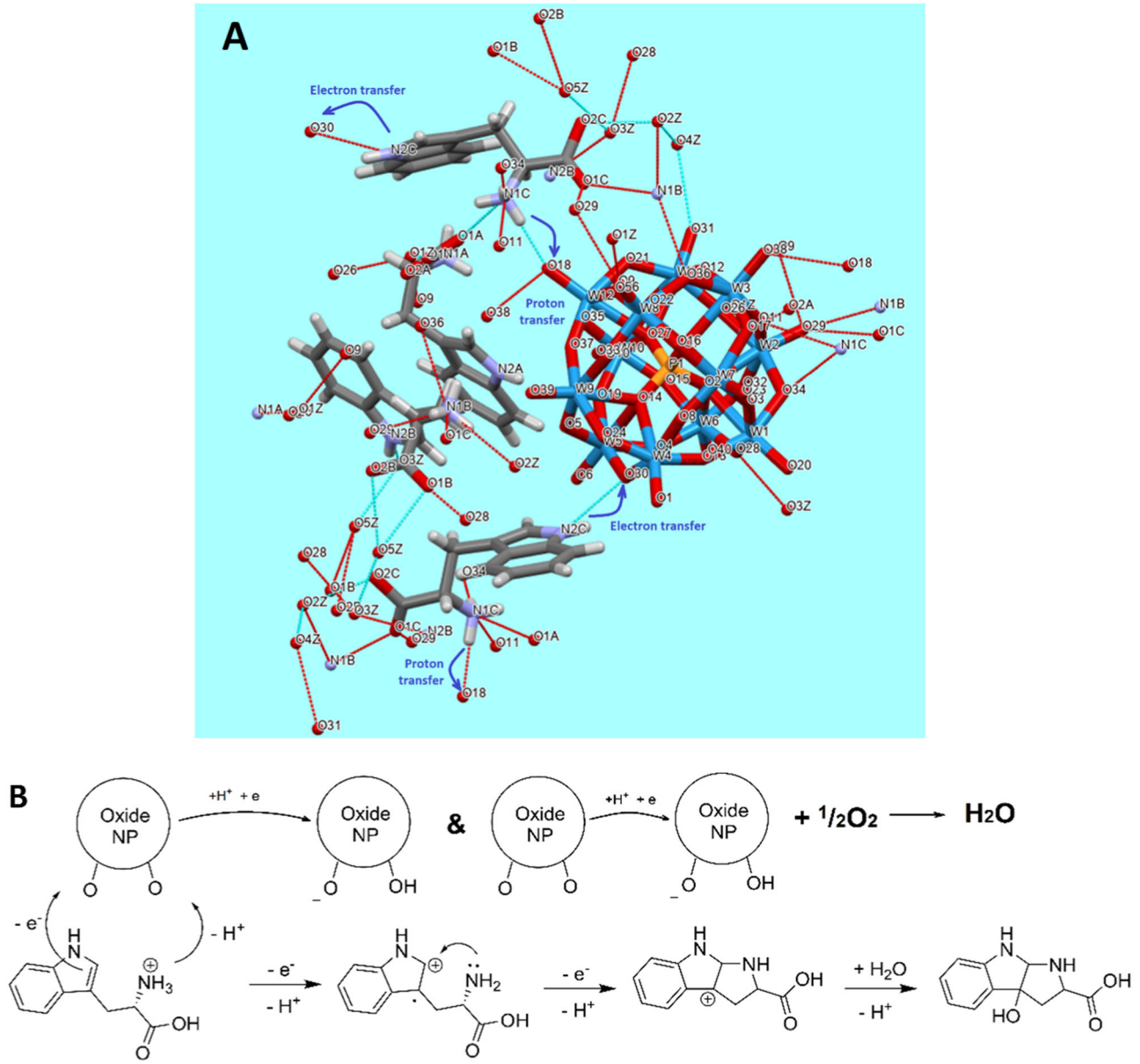

Fig. 6 Fragment of a crystal structure of POM-tryptophan complex, indicating the tracks of electron and proton transfer (**A**) and the discovered mechanism of direct specific tryptophan oxidation by NP (**B**) [37]

possible to demonstrate that both POM and NP with relatively high oxidation potentials were reacting with simultaneous proton and electron transfer, traced via interactions in the crystal structure between the tryptophan molecule and the POM and confirmed by a number of spectroscopic techniques and theoretical calculation (see Fig. 6) [37].

2.3 Modeling of single atom catalytic centers

Strong attention during the recent years has been attracted by the effects of single atom catalysts implanted on the surface of oxide matrices. Bringing understanding into placement of the doping atom and construction of its coordination sphere is challenging. Commonly applied techniques are indirect, using either photo luminescent characteristics of the inserted atom (being limited to structures with relatively good crystallinity/order and focusing very much on doping with RE elements [38]), or X-ray absorption spectroscopy approaches, such as EXAFS, requiring actually an in advance known reliable model for successful treatment of the data [39].

Principal breakthrough in providing such models has been made by the group of Dominic Wright at the University of Cambridge. They investigated interaction between transition metal halides and titanium and zirconium alkoxides under solvothermal conditions, leading to

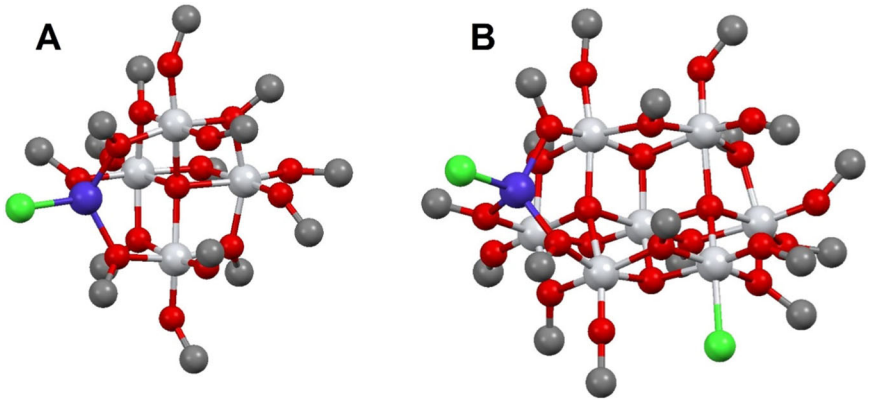

Fig. 7 Molecular structures demonstrating the $[Ti_4M^{II}O(OEt)_{15}Cl]$ (**A**) and $([Ti_7M^{II}O_5(OEt)_{18}Cl_2)]$ (**B**) arrangement types [40], M^{II} = Co, Ni, Fe, Zn. Only first carbon atoms of the ethyl groups are retained for clarity

multiple examples of surface-implanted titanium oxide related OAC structures. The most typical representatives of these species featured halide terminated penta-coordinated both early (as Cr(III) and Mn(II) and late transition element (Co(II), Ni(II), Cu(II), Zn(II)) atoms either capping a Ti_3O triangle as in $[Ti_4MO(OEt)_{15}Cl]$ (M = Co, Zn, Fe, Cu, see Fig. 7A), or replacing one of the peripheral Ti atoms in the Anderson POM like $Ti_7O_4(OEt)_{20}$ resulting in $[Ti_7M^{II}O_5(OEt)_{18}Cl_2)]$ (M^{II} = Co, Fe, see Fig. 7B) structures [40].

The observed structures permit to explain the enhanced reactivity of the surface-implanted transition metal atoms in the catalysts, because they feature lower coordination and are terminated by a halide atom that should be easy to substitute in surface reactions.

More recent attempts to use RE nitrate hydrate salts, $Ln(NO_3)_3{\cdot}xH_2O$, for implanting RE elements showed strong dependence on the Ti : RE molar ratio and thermal conditions. At lower Ti : RE ratios (about 2 : 1 and just above) at room temperature the crystallization of non-oxo species $[Ti_2Ln(O^iPr)_9(NO_3)_2]$ took place [41]. This structure is just the result of replacement of one Ti atom in the triangular aggregate, but with an alkoxide, not oxide ligand for charge compensation. Face-sharing octahedra with two Ti or zirconium atoms are stabilized in the presence of electropositive cations with large number of representatives of this structure type reported in literature [2]. More excitingly, at higher Ti : RE molar ratios, the result of interaction was dependent as noted above on the temperature conditions: at room temperature a salt of oligonuclear cation and anion, $[Ti_{12}(O^iPr)_{18}(\mu_3\text{-}O_{14})][La_3(NO_3)_{11}(HO^iPr)_6]$, was forming with a large yield, while on reflux conditions in the parent alcohol, ^{i}PrOH, a substituted MOP with the formula $[Ti_{11}La(O^iPr)_{17}(\mu_3\text{-}O)_{14}(NO_3)_2]$ was formed [42].

Getting insight into transition metal cation attachment to silica has also been investigated using alkoxide model species. In this case, the silsesquioxane molecules were used as models for silica surface and applied as ligands for metal alkoxides. Interestingly, it was discovered that even in

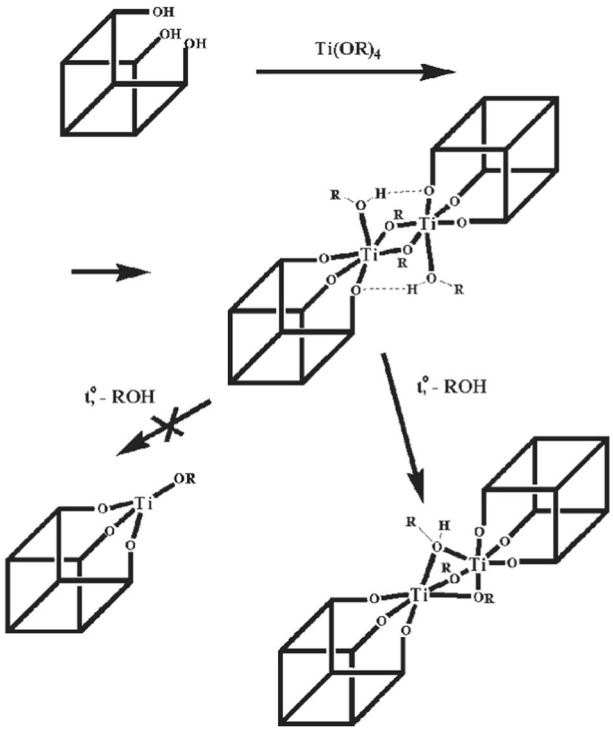

Fig. 8 Formation and thermal behavior of alkoxytitanasilsesquioxanes. Reprinted with permission from [43]

the excess of such ligands the transition metal fragments did not dissociate to single atoms, but remained a small group of even only two cations [43, 44]. These observations provided new insights into possible mechanisms of action of peroxidation catalysts in double C = C bond degradation (see Fig. 8).

2.4 Modeling of ligand surface attachment

Application of additional organic ligands in order to modify reactivity of metal alkoxides has gained popularity in 1980-es in connection to active development of metal oxide sol-gel for preparation of functional coatings and films [45].

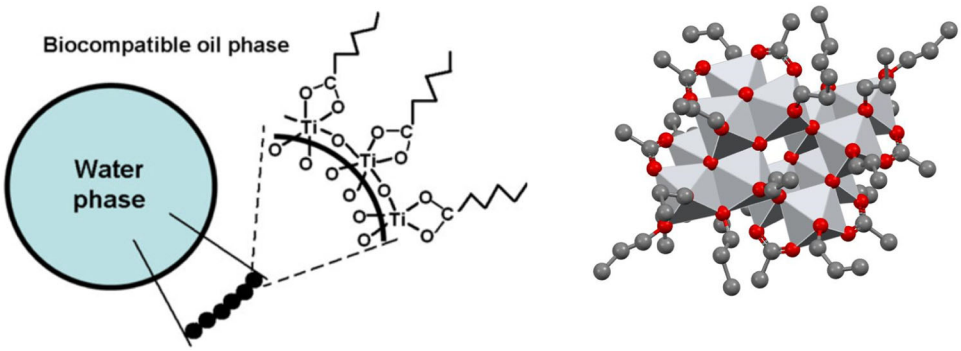

Fig. 9 The cartoon showing how long-chain heteroligands guide self-assembly of titania NP in an inverted Pickering emulsion (**A**) and the molecular structure of $Ti_{12}O_{12}(OAc)_6(O^nPr)_{18}$ polyhedral view (**B**). Reprinted with permission from [51]

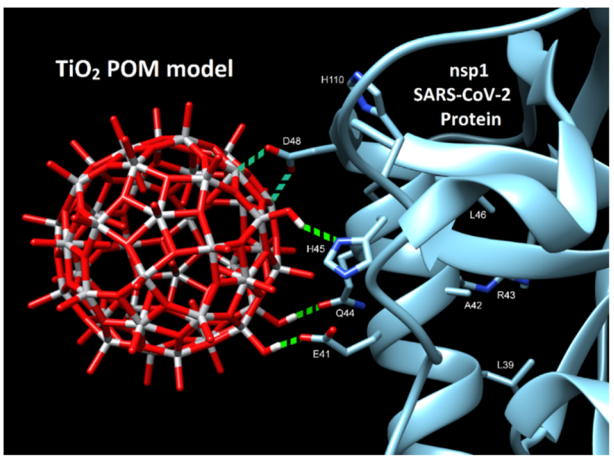

Fig. 10 Model showing the docking of the metal-oxygen core of $(H_6[Ti_{42}(\mu_3\text{-}O)_{60}(O^iPr)_{42}(OH)_{12})]$ with the structure of nsp1 taken from [62]. The possible interactions are show in cyan: carboxylate of D48 with titanium, forming an inner sphere complex, and green: hydrogen bonding of OH-groups from the nanoparticle to E41, Q44 and H45. The amino acids of the other amides showing chemical shift perturbation are marked. Reprinted with permission from [53]

Additional interest to these compounds emerged due to quest for single-source precursors of high-K dielectrics and High-Temperature Superconductors (HTSC), involving elements not producing soluble or volatile alkoxides, such as Cu, Pb etc. Sol-gel procedures to prepare HTSC and high-K dielectric layers were employing derivatives of other organic ligands than alkoxides for these elements together with alkoxides of Ti, Zr and RE elements, which resulted in isolation and structural characterization of a broad spectrum of so-called heteroleptic complexes [46]. Attachment modes of hetero ligands have in fact attracted a lot of attention from the very beginning, but were seen just in light of their binding into mixed-ligand complex molecules [47].

The interest in modeling the surface attachment of ligand to oxide NP emerged with growing applications of hybrid organic-inorganic materials and understanding of importance of insight into the activity of organic functions on the surface [48]. First steps were taken in the chemistry of silicon, where strong progress in characterization of oligomeric silsesquioxane compounds took place [49].

Most attractive goals in modeling with OAC turned to be the interaction of NP with biomolecules for, on one hand, biological and, specifically, drug delivery applications, and, on the other—understanding of possible interaction of NP with living cells and with viruses. Attachment modes and geometric parameters of bonding were obtained for many important classes of biological ligands. In particular, to understand the bonding and release mechanisms from titania NP the structures of titanium complexes with phenol family antibiotics like triclosan [50] were investigated. In order to understand self-assembly of surface-capped titania NP for encapsulation of time-temperature food indicators (Fig. 9A), the structures of carboxylate complexes were determined (Fig. 9B) [51]. Insight into bonding of oxy-carboxylate ligands such as lactate brought understanding for its stronger attachment to titania surface, hindering its interaction with proteins [52]. Among the most interesting results in application of OAC was discovery of the bonding mode of titania NP with proteins. It turned out that it occurs normally for not surface-protected TiO_2 NP via inner-sphere complexation with a carboxylic residue in a side-chain of an alpha-helix and requires to be supported by several strong hydrogen bonds to protonated amino groups of basic side chain residues (see Fig. 10) [53].

Very important class of biomolecules are those bearing phosphate residues that have extremely high affinity for metal oxide NP. Among examples of such classes are phospholipids, teichoic acid and nucleic acids, RNA and DNA. Interaction of phosphate residues with NP surface can effectively be modeled by investigation of molecular structures of complexes resulting from reactions of phosphonic acids with metal alkoxides. It was demonstrated that under near-neutral pH conditions the attachment of phosphate occurs in a tripodal fashion, binding to 3 different metal atoms, while under extremely acidic conditions one P-O-Ti bond can be broken due to protonation, resulting in a dipodal attachment. Connection of a phosphate/phosphonate

residue via only one oxygen atom has never been observed in the OAC models [54, 55].

2.5 Ligand effects on bandgap and hinders in modeling photocatalytic activity

One of the most exciting properties of metal oxide NP is their ability to act as photo catalysts producing reactive oxygen species for a broad spectrum of applications. The most addressed photo catalyst is titania, TiO_2, in its anatase phase [56]. It has, unfortunately, just a little too broad bandgap about 3.2 eV, which limits its efficiency to successfully using only the UV component of the visible light. It has been demonstrated, however, that ligands adsorbed/bound on the surface of titania NP can significantly change/reduce the bandgap. This can have many implications – from the use of surface-capped oxide NP in solar cells [55] and in photocatalytic water splitting [57] to possibilities in regulation of drug release from NP-containing composites [58]. OAC bearing relevant ligands can, via investigation of their optical characteristics, shed light on the influence of the attached molecules on the energy states in related titania NP. An important contribution to this field has been made by the group of Philip Coppens [34].

It is however, very important to bear in mind that OAC are not clusters, but paperbags. Attempts to measure their photocatalytic activity or adsorbent properties in aqueous medium result normally in measuring the activity of titania NP, to which they are converted by hydrolysis [55]. The literature contains quite a number of misinterpretations of this kind [59–61].

3 Conclusions

The idea of using metal alkoxides as models for metal oxides has through the four decennia after being originally formulated, developed into a powerful tool in modeling different characteristics of metal oxide NP. It offered insight into their bulk and especially surface structure, redox properties, surface reactivity etc. by visualizing the ligand attachment, and even providing clues to their electronic structure. A lot in this development has been driven by materials technology and especially nanotechnology.

Acknowledgements Financial support from the Swedish Research Council (Vetenskapsrådet) to the grant 2022-03971_VR, Molecular mechanisms in oxide nanoparticle interactions with proteins, is gratefully acknowledged. With deep gratitude to Professor Sumio Sakka for his constant interest and support of studies of metal alkoxide sol-gel precursors structure and reactivity.

Author contributions The sole author has composed this review on his own.

Funding Open access funding provided by Swedish University of Agricultural Sciences.

Compliance with ethical standards

Conflict of interest The author declares no competing interests.

Publisher's note Springer Nature remains neutral with regard to jurisdictional claims in published maps and institutional affiliations.

References

1. Bradley D, Mehrotar RC, Rothwell I, Singh A (2001) Alkoxo and aryloxo derivatives of metals, Elsevier, ISBN 0080488323, 9780080488325, https://doi.org/10.1016/B978-012124140-7/50005-0.
2. Turova NY, Turevskaya EP, Kessler VG, Yanovskaya MI (2002) The chemistry of metal alkoxides, Springer, ISSBN 978-0-7923-7521-0, 978-0-306-47657-0, https://doi.org/10.1007/b113856.
3. Sasai H, Suzuki T, Arai S, Arai T, Shibasa M (1992) Basic character of rare earth metal alkoxides. Utilization in catalytic C-C bond-forming reactions and catalytic asymmetric nitroaldol reactions. J Am Chem Soc 114:4418–4420. https://doi.org/10.1021/ja00037a068
4. Chisholm MH, Huffman JC, Kirkpatrick CC, Leonelli J, Folting K (1981) Metal alkoxides - models for metal oxides. 1. Preparations and structures of hexadecaalkoxytetratungsten compounds, W4(OR)16, where R = Me and Et, and octaoxotetraisopropoxytetrapyridinotetramolybdenum, Mo4(O)4(mu-O)2(mu3-O)2(O-i-Pr)2(mu-O-i-Pr)2(py)4. J Am Chem Soc 103:6093–6099. https://doi.org/10.1021/ja00410a018
5. Cahn JW, Taylor JE (1984) A contribution to the theory of surface energy minimizing shapes. Scr Metall 18:1117–1120. https://doi.org/10.1016/0036-9748(84)90189-3
6. Pauling L (1929) The principles determining the structure of complex ionic crystals. J Am Chem Soc 51:1010–1026. https://doi.org/10.1021/ja01379a006
7. Chisholm MH (2008) Frank Albert cotton. Biogr Mems Fell R Soc 54:95–115. https://doi.org/10.1098/rsbm.2008.0003
8. Kessler V (2023) Clusters or paperbags? What can we actually learn from the structure and reactivity of oligonuclear metal-oxo-alkoxide complexes? J Sol-Gel Si Technol https://doi.org/10.1007/s10971-023-06070-5.
9. Bradley DC (1967) Metal oxide alkoxide (trialkylsilyloxide) polymers. Coord Chem Rev 2:299–318. https://doi.org/10.1016/S0010-8545(00)80126-5

10. Edwards PG, Wilkinson G, Hursthouse MB, Abdul Malik KM (1980) Improved syntheses of tetrachloro-oxorhenium(VI) and chlorotrioxo-rhenium(VII). Synthesis of alkoxo- and dialkylamido-rhenium compounds. The crystal and molecular structures of di-μ-methoxo-tetramethoxo-μ-oxo-dioxodirhenium(VI)(Re–Re), bis[lithium pentaisopropoxo-oxorhenate(VI)–lithiumchloride–tetrahydrofuran(1/1/2)], and trans-tetraphenoxobis(trimethylphosphine)rhenium(IV). J Chem Soc Dalton Trans 2467-2475. https://doi.org/10.1039/DT9800002467.
11. Kessler VG, Seisenbaeva GA, Shevelkov AV, Khvorykh GV (1995) Synthesis, crystal, molecular and electronic structure of a novel heterobinuclear alkoxide cluster $[(MeO)_2ReO(\mu\text{-}OMe)_3MoO(OMe)_2]$. J Chem Soc Chem Comm 1779-1780. https://doi.org/10.1039/C39950001779.
12. Kessler V (2003) Molecular structure design and synthetic approaches to the heterometallic alkoxide complexes (soft chemistry approach to inorganic materials by the eyes of a crystallographer). Chem Commun 1213-1222. https://doi.org/10.1039/B209168M.
13. Seisenbaeva GA, Gohil S, Kessler VG (2004) Influence of heteroligands on the composition, structure and properties of homo- and heterometallic zirconium alkoxides. Decisive role of thermodynamic factors in their self-assembly. J Mater Chem 14:3177–3190. https://doi.org/10.1039/B404303K
14. Hampden-Smith MJ, Wark TA, Rheingold A, Huffman JC (1991) Solid state and solution structural investigation of homoleptic tin(IV) alkoxide compounds. Part I. $Sn(O\text{-}t\text{-}Bu)_4$ and $[Sn(O\text{-}i\text{-}Pr)_4 \cdot HO\text{-}i\text{-}Pr]_2$. Can J Chem 69:121–129. https://doi.org/10.1139/v91-02
15. Kessler VG, Mironov AV, Turova NY, Yanovsky AI, Struchkov YT (1993) The synthesis and X-ray crystal structure of molybdenum oxomethoxide $[MoO(OMe)_4]_2$. Polyhedron 12:1573–1576. https://doi.org/10.1016/S0277-5387(00)84601-X
16. Clegg W, Errington RJ, Kraxner P, Redshaw C (1992) Solid state and solution studies of Tungsten(VI) oxotetraalkoxides. J Chem Soc Dalton Trans 1431-1438. https://doi.org/10.1039/DT9920001431.
17. Day VW, Eberspacher TA, Chen YW, Hao JL, Klemperer WG (1995) Low-nuclearity titanium oxoalkoxides: the trititanates $[Ti_3O](OPri)_{10}$ and $[Ti_3O](OPri)_9(OMe)$. Inorg Chim Acta 229:391–405. https://doi.org/10.1016/0020-1693(94)04270-6
18. Spijksma GI, Seisenbaeva GA, Bouwmeester HJM, Blank DHA, Kessler VG (2013) Zirconium and hafnium tert-butoxides and tert-butoxo-β-diketonate complexes – Isolation, structural characterization and application in the one-step synthesis of 3D metal oxide nanostructures. Polyhedron 53:150–156. https://doi.org/10.1016/j.poly.2013.01.046
19. Zhang GY, Wang F, Tubul T, Baranov M, Leffler N, Neyman A, Poblet JM, Weinstock IA (2022) Complexed Semiconductor Cores Activate Hexaniobate Ligands as Nucleophilic Sites for Solar-Light Reduction of CO2 by Water. Angew Chem Int Ed 61:e202213162. https://doi.org/10.1002/anie.202213162
20. Spijksma GI, Seisenbaeva GA, Fischer A, Bouwmeester HJM, Blank DHA, Kessler VG (2009) The molecular composition of non-modified and acac-modified propoxide and butoxide precursors of zirconium and hafnium dioxides. J Sol-Jel Sci Technol 51:10–22. https://doi.org/10.1007/s10971-009-1988-0
21. Bradley DC, Hursthouse MB, Rodesiler PF (1968) The structure of a crystalline niobium oxide ethoxide, $Nb_8O_{10}(OEt)_{20}$. Chem Comm 1112-1113. https://doi.org/10.1039/C19680001112.
22. Boyle TJ, Sears JM, Perales D, Cramer RE, Lu P, Chan RO, Hernandez-Sanchez BA (2018) Synthesis and characterization of tris(trimethylsilyl)siloxide derivatives of early transition metal alkoxides that thermally convert to varied ceramic−silica architecture materials. Inorg Chem 57:8806–8820. https://doi.org/10.1021/acs.inorgchem.8b00630
23. Uchiyama H, Puthusseri D, Grins J, Gribble D, Seisenbaeva GA, Pol VG, Kessler VG (2021) Single-source alkoxide precursor approach to titanium molybdate, $TiMoO_5$, and its structure, electrochemical properties, and potential as an anode material for alkali metal ion batteries. Inorg Chem 60:3593–3603. https://doi.org/10.1021/acs.inorgchem.0c03087
24. Errington RJ, Petkar SS, Middleton PS, McFarlane W, Clegg W, Coxall RA, Harrington RW (2007) Non-aqueous synthetic methodology for TiW_5 polyoxometalates: protonolysis of $[(MeO)TiW_5O_{18}]^{3-}$ with alcohols, water and phenols. Dalton Trans 5211-5222. https://doi.org/10.1039/B709732H.
25. Gao MY, Wang F, Gu ZG, Zhang DX, Zhang L, Zhang J (2016) Fullerene-like polyoxotitanium cage with high solution stability. J Am Chem Soc 138:2556–2559. https://doi.org/10.1021/jacs.6b00613
26. Bemm U, Norrestam R, Nygren M, Westin G (1995) Preparation and structure of a manganese antimony mu5-Oxo ethoxide, Mn8Sb4(mu.5-O)4(mu3-OEt)4(mu-OEt)16. Inorg Chem 34:2367–2370. https://doi.org/10.1021/ic00113a017
27. Kessler VG, Seisenbaeva GA, Håkansson S, Unell M (2008) Chemically triggered biodelivery using metal-organic sol-gel synthesis. Angew Chem Int Ed 44:8506–8509. https://doi.org/10.1002/anie.200803307
28. Seisenbaeva GA, Daniel G, Nedelec JM, Kessler VG (2013) Solution equilibrium behind room temperature synthesis of nanocrystalline titanium dioxide. Nanoscale 5:3330–3336. https://doi.org/10.1039/C3NR34068F
29. Starikova ZA, Kessler VG, Turova NY, Tcheboukov DE, Suslova EV, Seisenbaeva GA, Yanovsky AI (2004) New polynuclear aluminium oxoalkoxides: molecular structures of $Al_{11}(\mu_4\text{-}O)_2(\mu_3\text{-}O)_2(\mu\text{-}O)_2(\mu\text{-}OPr^n)_{10}(\mu\text{-}OPr^i)_2(\mu\text{-}ROH)_2(OPr^i)_8(OR)$, $R{=}Pr^{n,i}$ and $Al_5Mg_4(\mu_4\text{-}O)_2(\mu_3\text{-}O)(\mu\text{-}OH)_3(\mu\text{-}OPr^i)_8(\mu,\eta^2\text{-}acac)_4(\eta^2\text{-}acac)_2$. Polyhedron 23:109–114. https://doi.org/10.1016/j.poly.2003.09.031
30. Seisenbaeva GA, Gohil S, Suslova EV, Rogova TV, Turova NY, Kessler VG (2005) The synthesis of iron (III) ethoxide revisited: Characterization of the metathesis products of iron (III) halides and sodium ethoxide. Inorg Chim Acta 358:3506–3512. https://doi.org/10.1016/j.ica.2005.03.048
31. Helgesson G, Jagner S, Poncelet O, Hubert-Pfalzgraf LG (1991) Synthesis and molecular structure of $Nd_5(\mu_5\text{-}O)(\mu_3\text{-}OR)_2(\mu_2\text{-}OR)_6(OR)_5(ROH)_2$ ($R = Pr^i$). The first example of a trigonal bipyramidal metal oxoalkoxide. Polyhedron 10:1559–1564. https://doi.org/10.1016/S0277-5387(00)86080-5
32. Turova NY, Turevskaya EP, Kessler VG, Yanovsky AI, Struchkov YT (1993) Synthesis, crystal and molecular structure of calcium oxo ethoxide, $[Ca_6(\mu_4\text{-}O)_2(\mu_3\text{-}OEt)_4(OEt)_4]\cdot 14EtOH$. J Chem Soc Chem Commun 21-23. https://doi.org/10.1039/C39930000021.
33. Suslova EV, Turova NY, Kessler VG, Belokon' AI (2007) Electrosynthesis of tin(II) alkoxides. Coor Comp 52:1682–1686. https://doi.org/10.1134/S0036023607110083
34. Coppens P, Chen YF, Trzop E (2014) Crystallography and properties of polyoxotitanate nanoclusters. Chem Rev 114:9645–9661. https://doi.org/10.1021/cr400724e
35. Chisholm MH, Huffman JC, Leonelli J, Rothwell IP (1982) Metal alkoxides: models for metal oxides. 3. Further studies of the carbonylation of hexaalkoxides of dimolybdenum and ditungsten (M.tplbond.M) and characterization of M2(O-i-Pr)6(py)2(μ-CO) (M:M) compounds. J Am Chem Soc 104:7030–7036. https://doi.org/10.1021/ja00389a024
36. Mahmoudi M, Landry MP, Moore A, Coreas R (2023) The protein corona from nanomedicine to environmental science. Nat Rev Mater 8:422–438. https://doi.org/10.1038/s41578-023-00552-2
37. Nefedova A, Svensson FG, Vanetsev AS, Agback P, Agback T, Gohil S, Kloo L, Tätte T, Ivask A, Seisenbaeva GA, Kessler VG

(2024) Molecular Mechanisms in Metal Oxide Nanoparticle –Tryptophan Interactions. Inorg Chem 63:8556–8566. https://doi.org/10.1021/acs.inorgchem.3c03674
38. Cojocaru B, Avram D, Kessler V, Parvulescu V, Seisenbaeva G, Tiseanu C (2017) Nanoscale insights into doping behavior, particle size and surface effects in trivalent metal doped SnO2. Sci Rep. 7:9598. https://doi.org/10.1038/s41598-017-09026-2
39. Iglesias-Juez A, Chiarello GL, Patience GS, Guerrero-Pérez MO (2022) Experimental methods in chemical engineering: X-ray absorption spectroscopy—XAS, XANES, EXAFS. Can J Chem Eng 100:3–22. https://doi.org/10.1002/cjce.24291
40. Eslava S, Goodwill BPR, McPartlin M, Wright DS (2011) Extending the family of titanium heterometallic–oxo–alkoxy cages. Inorg Chem 50:5655–5662. https://doi.org/10.1021/ic200350j
41. Svensson FG, Cojocaru B, Qiu Z, Parvulescu V, Edvinsson T, Seisenbaeva GA, Tiseanu C, Kessler VG (2021) Rare-earth-modified titania nanoparticles: molecular insight into synthesis and photochemical properties. Inorg Chem 60:14820–14830. https://doi.org/10.1021/acs.inorgchem.1c02134
42. Fang WH, Li H, Lv YK, Wright DS (2021) A cocrystallization of polyoxotitanium cages with lanthanide clusters. J Solid State Chem 294:121852. https://doi.org/10.1016/j.jssc.2020.121852
43. Viotti O, Seisenbaeva GA, Kessler VG (2009) Tripodal tetrahedral titanium coordination in the silica-grafted titania epoxidation catalysts: is not it only a myth? selective formation of [Cy7Si7O12Ti]2(μ-OR)2(μ-ROH) cores on thermal "dissociation" of alkoxytitanasilsesquioxanes. Inorg Chem 48:9063–9065. https://doi.org/10.1021/ic901503y
44. Viotti O, Fischer A, Seisenbaeva GA, Kessler VG (2010) Straightforward synthesis and structural characterization of the first alkoxy-zircono-silsesquioxanes - potential models for binding of zirconium cations to silica matrices in epoxidation catalysts. Inorg Chem Comm 13:774–777. https://doi.org/10.1016/j.inoche.2010.03.044
45. Livage J, Sanchez C, Henry M (1988) Sol-gel chemistry of transition metal oxides. Prog Solid State Chem 18:259–341. https://doi.org/10.1016/0079-6786(88)90005-2
46. Hubert-Pfalzgraf LG (2003) Some trends in the design of homo- and heterometallic molecular precursors of high-tech oxides. Inorg Chem Comm 6:102–120. https://doi.org/10.1016/S1387-7003(02)00664-0
47. Schubert U (2005) Chemical modification of titanium alkoxides for sol–gel processing. J Mater Chem 15:3701–3715. https://doi.org/10.1039/B504269K
48. Judeinstein P, Sanchez C (1996) Hybrid organic–inorganic materials: a land of multidisciplinarity. J Mater Chem 6:511–525. https://doi.org/10.1039/JM9960600511
49. Takahashi N, Kuroda K (2011) Materials design of layered silicates through covalent modification of interlayer surfaces. J Mater Chem 21:14336–14353. https://doi.org/10.1039/C1JM10460H
50. Svensson F, Seisenbaeva GA, Kessler VG (2017) Mixed-ligand titanium "Oxo Clusters": structural insights into the formation and binding of organic molecules and transformation into oxide nanostructures on hydrolysis and thermolysis. Eur J Inorg Chem 4117-4122. https://doi.org/10.1002/ejic.201700775.
51. Seisenbaeva GA, Ilina E, Håkansson S, Kessler VG (2010) A new concept for titanium oxo-alkoxo-carboxylates' encapsulated biocompatible time temperature food indicators based on arising, not fading color. J Sol-Gel Sci Techol 55:1–8. https://doi.org/10.1007/s10971-010-2195-8
52. Svensson FG, Manivel VA, Seisenbaeva GA, Kessler VG, Nilsson B, Ekdahl KN, Fromell K (2021) Hemocompatibility of nanotitania-nanocellulose hybrid materials. Nanomaterials 11:1100. https://doi.org/10.3390/nano11051100
53. Agback P, Agback T, Dominguez F, Frolova E, Seisenbaeva GA, Kessler VG (2022) Site-specific recognition of SARS-CoV-2 nsp1 protein with a tailored titanium dioxide nanoparticle–elucidation of the complex structure using NMR data and theoretical calculation. Nanoscale Adv 4:1527–1532. https://doi.org/10.1039/D1NA00855B
54. Seisenbaeva GA, Melnyk IV, Hedin N, Chen Y, Eriksson P, Trzop E, Zub YL, Kessler VG (2015) Molecular insight into the mode-of-action of phosphonate monolayers as active functions of hybrid metal oxide adsorbents. Case study in sequestration of rare earth elements. RSC Adv 5:24575–24585. https://doi.org/10.1039/C4RA15531A
55. Svensson FG, Daniel G, Tai CW, Seisenbaeva GA, Kessler VG (2020) Titanium phosphonate oxo-alkoxide "clusters": solution stability and facile hydrolytic transformation into nano titania. RSC Adv 10:6873–6883. https://doi.org/10.1039/C9RA10691J
56. Nakata K, Fujishima A (2012) TiO2 photocatalysis: design and applications. J Photochem Photobio C: Photochem Rev 13:169–189. https://doi.org/10.1016/j.jphotochemrev.2012.06.001
57. Sari Y, Lobo Gareso P, Armynah B, Tahir D (2024) A review of TiO_2 photocatalyst for organic degradation and sustainable hydrogen energy production. Int J Hydrog Energy 55:984–996. https://doi.org/10.1016/j.ijhydene.2023.11.126
58. Galkina OL, Önneby K, Huang P, Ivanov VK, Agafonov AV, Seisenbaeva GA, Kessler VG (2015) Antibacterial and photochemical properties of cellulose nanofibers–titania nanocomposites loaded with two different types of antibiotic medicines. J Mater Chem B 3:7125–7134. https://doi.org/10.1039/C5TB01382H
59. Zhu BC, Hong QL, Yi XF, Zhang J, Zhang L (2020) Supramolecular co-assembly of the Ti_8L_{12} Cube with $[Ti(DMF)_6]$ species and Ti_{12}-oxo cluster. Inorg Chem 59:8291–8297. https://doi.org/10.1021/acs.inorgchem.0c00682
60. Zhang K, Du SW (2021) Studies of high-nuclearity lanthanide-titanium oxo clusters: Structure and properties. Inorg Chim Acta 528:120621. https://doi.org/10.1016/j.ica.2021.120621
61. Ge CY, Hou JL, Zhou ZY, Zhu QY, Dai J (2022) A cyclic titanium-oxo cluster with a tetrathiafulvalene connector as a precursor for highly efficient adsorbent of cationic dyes. Inorg Chem 61:486–495. https://doi.org/10.1021/acs.inorgchem.1c03161
62. Clark LK, Green TJ, Petit CM (2021) Structure of nonstructural protein 1 from SARS-CoV-2. J Virol 95:e02019. https://doi.org/10.1128/jvi.02019-20